

**Received:** 2006.04.24  
**Accepted:** 2006.10.21  
**Published:** 2006.12.22

## Assessment of different MCNP Monte Carlo codes in electron absorbed dose

### Authors' Contribution:

- A** Study Design
- B** Data Collection
- C** Statistical Analysis
- D** Data Interpretation
- E** Manuscript Preparation
- F** Literature Search
- G** Funds Collection

**Hassan Ali Nedaie<sup>1,2</sup>, M. A. Mosleh-Shirazi<sup>2,3</sup>, H Gharraati<sup>1</sup>, M. Shariari<sup>4</sup>, M. Allahverdi<sup>1</sup>**

<sup>1</sup> Radiotherapy Physics Department, Cancer Research Centre, Cancer Institute, Tehran University of Medical Sciences, Tehran, Iran

<sup>2</sup> Joint Department of Physics, Royal Marsden Hospital and Institute of Cancer Research, Sutton, Surrey, U.K.

<sup>3</sup> Department of Radiotherapy, Namazi Hospital, Shiraz University of Medical Sciences, Shiraz, Iran

<sup>4</sup> Department of Nuclear Engineering, Shahid Beheshti University, Tehran, Iran

### Summary

#### Background

MCNP is a general-purpose Monte Carlo code for simulation of neutrons, photons and electrons or coupled neutron/photon/electron transport. This code is based on ETRAN/ITS codes. There are different versions of this code.

#### Aim

This work aims to compare the more recently released MCNP codes with the earlier version in terms of the central axis absorbed dose (CADD), the energy spectrum and the computational efficiency. MCNP codes 4A, 4B, 4C, X and 5 were compared for a 10MeV electron beam in water.

#### Materials/Methods

The energy spectra of electrons were scored on the phantom surface and planes 3 and 5cm deep using F2 tally subdivided into 0.1MeV energy bins. This tally also was repeated for 4A, 4B, 4C and X with smaller energy bins (0.05MeV). The simulated geometry and other input parameters were kept the same. Both the default and ITS energy indexing algorithms (EIA) were used in 4B, 4C and X, while only the default EIA was employed in 4A and 5.

#### Results

With default indexing, X and 5 showed no difference in CADD compared to 4B and 4C and were within 3% of 4A. We found no differences in CADD between codes when 4B, 4C and X were used with ITS indexing. The ITS algorithm improved computational efficiency. For the energy spectrum at the phantom surface, all codes except X show very similar results (within 2%). However, changing the energy indexing to ITS as well as using a 0.05MeV bin removed this discrepancy at the surface for X code.

#### Conclusions

While, under the examined conditions, versions 4B and later behaved similarly in terms of the resulting CADD, the ITS indexing should be used due to its agreement with measurements and computational efficiency.

#### Key words

**radiotherapy • electron therapy • Monte Carlo • absorbed dose • energy spectrum**

**Full-text PDF:** <http://www.rpor.pl/pdf.php?MAN=9888>  
**Word count:** 1747  
**Tables:** 1  
**Figures:** 6  
**References:** 13

**Author's address:** Hassan Ali Nedaie, Radiotherapy Physics Department, Cancer Institute, Tehran University of Medical Sciences, Tehran, Iran, e-mail: nedaieha@sina.tums.ac.ir

## BACKGROUND

Monte Carlo (MC) techniques are becoming more widely used in all medical physics applications. MC simulation of radiation transport is considered a highly accurate method of radiation therapy dose calculation. There are different MC codes for simulation of photons, electrons and the coupled transport of electrons and photons. There are three main families of MC codes frequently used for modelling of electron beams: ETRAN/ITS [1,2], EGS4 [3] and PENELOPE [4]. The MCNP code is based on the ETRAN/ITS electron transport system.

The MCNP-4A electron physics is based on version 1.0 of the ITS code system but 4B and later codes use the electron physics of ITS version 3.0. There are two major improvements in ITS 3.0 compared to ITS 1.0. First, the accuracy of the tabulation and sampling of the Landau energy straggling distribution was improved by using Landau's universal function. Second, an improvement in the Blunk-Leisegang correction to the Landau distribution led to more accurate simulation of electron transport at lower energies and in higher atomic number media [5].

The main improvements in 4C relevant to electron transport were in density effect calculation for stopping power, radiative stopping power and Bremsstrahlung production as well as a new electron library (E103). MCNP-X (version 2.4.0, released in 2002) includes extensions to higher energies and more particle types but uses the same library as 4C for electron transport. MCNP-5, released in 2003, also uses the same electron libraries as 4C and includes the addition of nuclear collision physics.

In MCNP, all pre-calculated and tabulated data for electrons are stored on an energy grid. MCNP offers two energy indexing algorithms that determine the data from which energy group is used: the default MCNP energy indexing algorithm or the ITS energy indexing. The default indexing uses the data in which the energy of the electron lies somewhere between the group boundaries,

but the ITS indexing uses the data from the group whose boundary is closest to the energy of the electron at the beginning of the step [6,7]. These two indexing algorithms are also called "bin centred" and "nearest group boundary" treatments.

Published papers on MCNP electron transport have covered up to version 4C. Love et al. [8] used EGS4 and MCNP-4A and 4B to calculate central axis depth doses (CADDs) in water for a 10MeV electron beam. Jeraj et al. [6] showed that when MCNP-4B was run in the default mode, lower surface dose and deeper penetration was observed compared with EGS4. When the ITS energy-indexing scheme was used, EGS4 and MCNP-4B agreed with each other within the statistical uncertainty of the calculations. There was a good agreement between experimental electron depth dose distributions with EGS4 and MCNP-4B results but a discrepancy of 10% of the maximum dose when MCNP-4A was used. Edwards and Mountford [9] found that a shorter computation time was required for 4A compared to 4B to obtain the same results for electron beams. Wang and Li [10] reported differences of up to 30% between beta dose distributions calculated using MCNP-4B, EGS4 and EGSnrc codes. The results obtained by Cross et al. [11] for a concave Ru-106 eye applicator with ACCEPT 3.0, one of the ITS 3.0 codes, showed good agreement with experimental measurements, while MCNP-4B results were different. Chibani and Li [12] compared the results between GEPTS, EGSnrc, MCNP-4C and measurements and found that the differences between the results of GEPTS and EGSnrc for almost all energies and media were very small but MCNP results depended significantly on the electron energy indexing method. Schaart et al. [7] observed discrepancies between ITS 3.0 and MCNP-4C, although the same electron transport algorithms were used in both codes.

## AIM

This work aims to compare the more recently released MCNP codes with the earlier version in

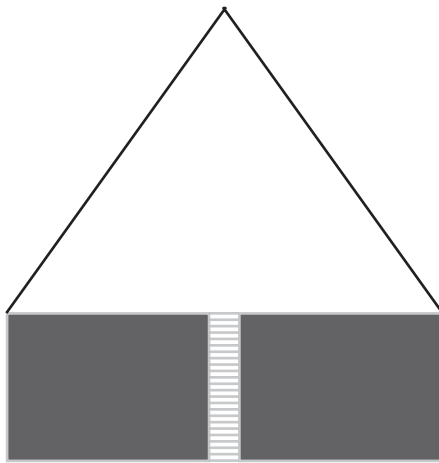


**Figure 1.** Diagram of the simulated phantom and point source.

terms of the CADD in water, the energy spectrum at three different levels in the phantom and computation time. MCNP codes 4A, 4B, 4C, X and 5 (versions 1.2 and 1.3) were studied.

## MATERIALS AND METHODS

Monoenergetic electrons with a nominal energy of 10MeV were modelled.  $10^6$  source particles were simulated each time. The geometry used to produce the CADD curves consisted of a conical electron beam originating from a point source and impinging on a water phantom at 100cm SSD (Figure 1). The water phantom had a  $20 \times 20 \text{ cm}^2$  cross-sectional area and was 10cm deep. A 1cm radius concentric cylinder defined the dose-scoring region on the central axis. This geometry uses the geometry-equivalence or reciprocity theorem [13] to offer better variance reduction and therefore speed improvements. Other variance reduction methods were not used. The smaller cylinder was divided into 50 slabs of 0.2cm thickness to show detail in the build-up region. The electron energy cut-off was 0.5MeV while photons were transported down to the energy of 100keV. In order to ensure that the value of the electron energy cut-off used was not too high, the CADD was also obtained without a cut-off.

Both the ITS and default energy indexing algorithms were used in 4B, 4C and X, while only the default algorithm was employed in 4A and 5. All calculations were carried out in coupled electron-photon mode [MODE P E]. The energy deposited in each of these cells was scored by means of \*F8 tally. To obtain the absorbed dose,

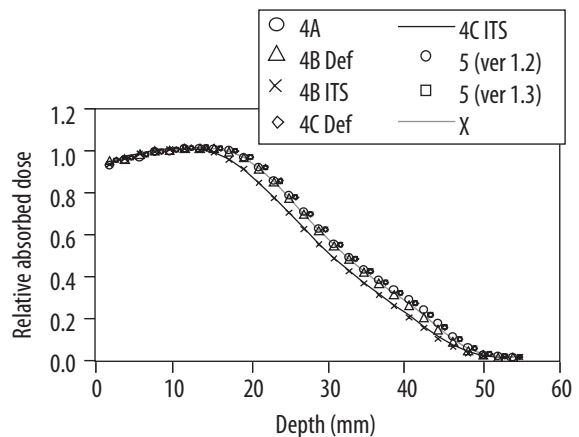


**Figure 2.** Central axis depth dose curves computed using MCNP-4A, 4B, 4C, X and 5 codes.

all of the energy deposited in each cell was divided by the cell mass.

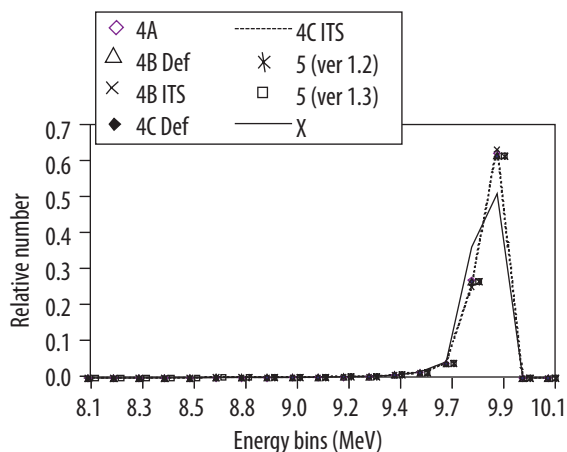
The energy spectra of electrons were scored on the phantom surface and planes 3 and 5cm deep using F2 tally subdivided into 0.1MeV energy bins. This tally also was repeated for 4A, 4B, 4C and X with smaller energy bins (0.05MeV). The scoring area was  $50 \text{ cm}^2$ .

We have been unable to make a direct comparison of the computational efficiency of the codes using the same computer due to practical constraints. MCNP-4A and 4B ran under the Windows 98 operating system (OS) on computer A (2x2 GHz CPU, 512 MB RAM). MCNP-4C ran under Windows XP OS on the same computer. MCNP-5 ran under Windows 2000 OS on computer B (750 MHz CPU, 2 GB RAM) and MCNP-X ran under Windows XP OS on computer C (2.8 GHz CPU, 256 MB RAM).

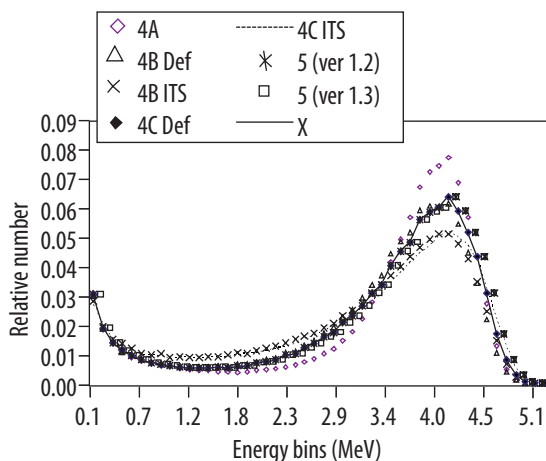
## RESULTS

Figure 2 shows CADD curves for all six codes together. The statistical uncertainty in the CADD values ranged between 0.002% and 0.01% depending on depth. The simulation with 4C repeated with no electron energy cut-off produced negligible differences (mean =0.01%, maximum =0.04%).

The energy spectra at the three planes are shown in Figures 3–6. Each plotted point was obtained by dividing the energy bin count by the total number at that plane. For the energy spectrum at the phantom surface (Figure 3), all codes except



**Figure 3.** Energy spectrum for MCNP-4A, 4B, 4C, X and 5 codes at the phantom surface with 0.1MeV energy bins.



**Figure 5.** Energy spectrum for MCNP-4A, 4B, 4C, X and 5 codes at 3cm depth with 0.1MeV energy bins.

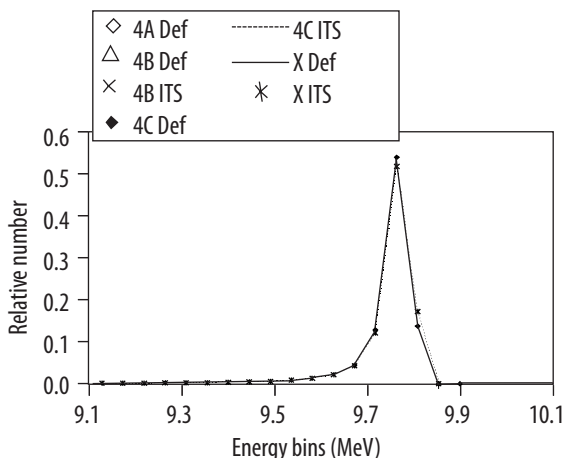


**Figure 4.** Energy spectrum for MCNP-4A, 4B, 4C and X codes at the phantom surface with 0.05MeV energy bins.

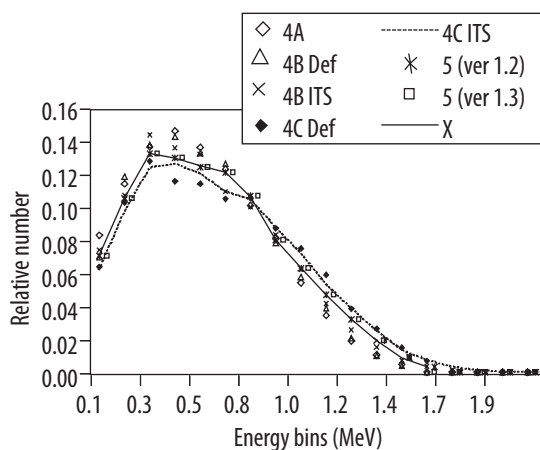


**Figure 6.** Energy spectrum for MCNP-4A, 4B, 4C, X and 5 codes at 5cm depth with 0.1MeV energy bins.

X show very similar results (within 2%). However, changing the energy indexing to ITS as well as using a 0.05MeV bin removed this discrepancy at the surface for X code. The only differences were displaying the contrast between ITS and default modes when 0.05MeV energy bin was used. On the other hand, using smaller energy bins reveals contrast at the phantom surface for two modes (Figure 4). At greater depths (Figures 5, 6), there are greater differences between the codes. At the 3cm deep plane, codes 4B, 4C default, X and 5 are within 1% of each other, while 4A gives a 19% greater peak value and 4B and 4C ITS indexing are 16% lower. Repeating with 0.05MeV energy bin showed similar results for 3cm and 5cm deep planes. The range in statistical uncertain-

ty in energy spectrum was 0.004–0.012% at the surface, 0.01–0.05% at 3cm depth and 0.2–0.7% at 5cm depth.

Table 1 shows the different computer run times for all codes on the corresponding computers for  $10^6$  histories. The ITS indexing takes a 22% shorter run time compared to the default. Although running on different computers, our results suggest a shorter computation time for 4C and X compared to the others.

**DISCUSSION AND CONCLUSIONS**

When using the default energy indexing, the more recent codes (X and 5) showed no difference in

**Table 1.** Computer Run time for 10<sup>6</sup> particles.

MCNP Codes	Energy index algorithm	Computer run time (minutes)
4A	Default	687 (Computer A)
4B	Default	737 (Computer A)
4B	ITS	576 (Computer A)
4C	Default	512 (Computer A)
4C	ITS	396 (Computer A)
X	Default	640 (Computer C)
5 (ver 1.2)	Default	1242 (Computer B)
5 (ver 1.3)	Default	1237 (Computer B)

CADD compared to 4B and 4C and were within 3% of 4A. The difference in the results from 4A can be attributed to the use of different electron physics data (ITS 1.0). We found no differences in CADD between 4B and 4C when using the same indexing. Our results show that the indexing algorithm (rather than the choice of code) governs the depth dose curve and the change of version by itself has a negligible effect.

There were differences of up to 10–15% in absorbed dose results between the default and ITS indexing. The more rapid dose deposition with the ITS indexing leads to a shorter electron range. Similar differences have also been reported by Jeraj et al. [6] and Schaart et al. [7].

The choice of indexing algorithm had a negligible effect on the energy spectrum at the surface of the phantom but had a greater effect within it. In spite of X using the same electron library as the other codes (except 4A), energy spectra in this code are different from the others at the surface of the phantom with 0.1MeV energy bins. By using smaller energy bins this discrepancy disappears and the only difference concerns the contrast between ITS and default mode, which requires further investigation. However, the differences between the energy spectra of X and the others in 0.1MeV energy bin disappear at the other planes within the phantom.

ITS indexing resulted in a shorter computation time compared to the default. 4C required a shorter time than 4B and 4A. Our results are in general agreement with the work of Edward and Mountford [9] showing a shorter computation time for 4A compared to 4B in electron transport. Our results suggest a shorter run time for 4C and X compared to the others.

Previous works [6] have shown that the results of 4B (ITS) agree with experimental measure-

ments. We have shown that 4C produces very similar CADD values to 4B. We have also observed the same for X (ITS) (data not shown). These results indicate that, under the examined conditions, codes 4B and later behave similarly in terms of the resulting depth dose characteristics. The ITS indexing algorithm should be used in preference due to its agreement with measurements and computational efficiency. However, the trends for energy spectrum are not as clear and require further investigation as well as other electron energies and more complex geometries.

#### ACKNOWLEDGMENTS

We are grateful to Jon Cox, who ran the MCNP-5 simulations in Los Alamos National Laboratory.

#### REFERENCES:

1. Halbleib H: Structure and operation of the ITS code system, in Monte Carlo transport of electrons and photons, Jenkins TM, Nelson WR, Rindi A et al (editors), New York: Plenum, 1988; 249–62
2. Seltzer SM: An overview of ETRAN Monte Carlo methods, in Monte Carlo transport of electrons and photons, edited by Jenkins TM, Nelson WR, Rindi A et al (editors), New York: Plenum, 1988; 153–82
3. Nelson WR, Hirayama H, Royans DW: The EGS4 code System, Stanford linear accelerator centre (SLAC), Report, 1985; 265
4. Baro J, Sempau J, Fernandez-Vera JM et al: PENELOPE: an algorithm for Monte Carlo simulation of the penetration and energy loss of electrons and positron in matter. Nucl Inst Meth, 1995; 31–46
5. Halbleib JA, Kensek RP, Valdez GD et al: ITS the Integrated Tiger Series of electron/Photon Transport Codes – ver 3.0. Nucl Sci, 1992; 39: 1025–9
6. Jeraj R, Keal PJ, Ostwald PM: Comparisons between MCNP, EGS4 and experiment for clinical electron

- beams. *Phys Med Biol*, 1999; 44: 705–17
7. Schaart DR, Jansen JT, Zoeteliff J et al: A Comparison of MCNP4C electron transport with ITS 3.0 and experiment of incident energy between 100keV and 20MeV. *Phys Med Biol*, 2002; 47: 1459–84
  8. Love PA, Lewis DG, Affan AM et al: Comparison of EGS4 and MCNP Monte Carlo codes when calculating radiotherapy depth doses. *Phys Med Biol*, 1998; 43: 1351–57
  9. Edward CR, Mountford PJ: The X-ray and electron benchmarking of the Monte Carlo codes MCNP-4A and 4B on different computers. *Br J Radiol*, 1999; 72: 196–200
  10. Wang R, Li XA: Monte Carlo dose Calculation of beta – emitting sources for intravascular brachytherapy: A comparison between EGS4, EGS/nrc and MCNP. *Med Phys*, 2001; 28: 134–41
  11. Cross WG, Hokkanen J, Jarvinen H et al: Calculation of beta ray dose distribution from ophthalmic applicators and comparison with measurement in a model eye. *Med Phys*, 2001; 28: 1385–96
  12. Chaibani O, Li XA: Monte Carlo dose calculation in homogenous media and at interfaces: A comparison between GEPTS, EGSnrc, MCNP, and measurements. *Med Phys*, 2002; 29: 835–47
  13. ICRU. Radiation dosimetry: electron beams with energies between 1 and 50MeV ICRU report 35, Bethesda, MD: ICRU, 1984